Electron Transfer Mechanisms upon Lithium Deintercalation from $LiCoO_2$ to CoO_2 Investigated by XPS

L. Dahéron,[†] R. Dedryvère,*[,†] H. Martinez,[†] M. Ménétrier,[‡] C. Denage,[‡] C. Delmas,[‡] and D. Gonbeau[†]

IPREM/ECP, Université de Pau, Hélioparc Pau Pyrénées, 2 av. Pierre Angot, 64053 Pau cedex 9, France, and ICMCB, CNRS, Université Bordeaux I, 87 av. du Dr A. Schweitzer, 33608 Pessac cedex, France

Received September 6, 2007. Revised Manuscript Received November 15, 2007

Lithium deintercalation of Li_xCoO_2 from $x = 1$ to $x \approx 0$ has been carried out electrochemically. The changes in the electronic structure from $LiCoO_2$ to CoO_2 have been investigated by X-ray photoelectron spectroscopy (XPS) to bring some new developments about the electron transfer mechanisms upon lithium deintercalation. All available XPS core peaks (Co 2p, Co 3p, Co 3s, O 1s, F 1s, P 2p, C 1s) and valence spectra have been analyzed. The contributions of the electrode material and of the electrode/electrolyte interface have been clearly distinguished. We show that cobalt and oxygen simultaneously undergo a partial oxidation process and that the sole participation of oxygen atoms to the charge transfer process, as it is sometimes assumed, can be excluded. The surface film consists of organic and inorganic species resulting from degradation of the electrolyte.

Introduction

$LiCoO_2$ is a compound of great importance as it is the most widely used positive electrode material of today's lithium ion batteries. The reason for this success is that Li^+ ions can be deintercalated from $LiCoO_2$ down to $Li_{0.5}CoO_2$ with a very good reversibility and a high electrochemical potential (up to 4.2 V vs Li^+/Li), giving rise to batteries with a good cyclability and a high voltage.[1,2] $LiCoO_2$ crystallizes in the rhombohedral system (space group $R\bar{3}m$) with the α-$NaFeO_2$-type structure. This layered structure, named O3, can be represented as an ordered rocksalt type with an ABCABC stacking of oxygen planes, with the Li^+ and Co^{3+} ions ordered in alternate layers of octahedral sites of the (111) planes.[3] The lithium ions can reversibly deintercalate from the van der Waals gap between CoO_2 layers.

Numerous reports have elucidated the phase changes upon lithium deintercalation from Li_xCoO_2, which undergoes only small structural changes for $0.3 \leq x \leq 1$.[4–6] Figure 1 shows the first galvanostatic charge/discharge curve of an Li_xCoO_2/Li electrochemical cell (C/20 rate, i.e., one Li intercalated/deintercalated in 20 h). The $0.94 \leq x \leq 1$ domain corresponds to a solid solution. The voltage plateau observed for $0.75 \leq x \leq 0.94$ corresponds to a two-phase region

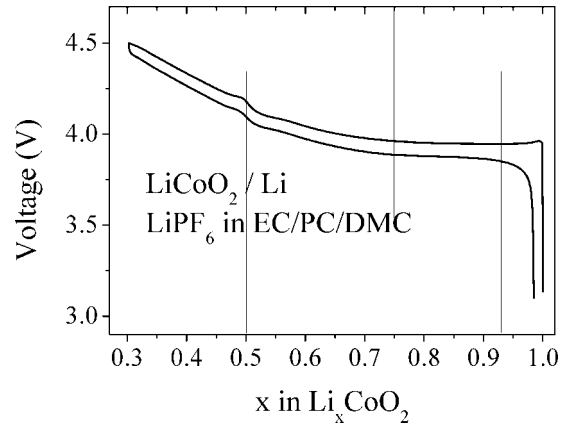

Figure 1. First galvanostatic charge/discharge curve of a Li_xCoO_2/Li electrochemical cell.

induced by an insulator–metal transition.[7] Indeed, $LiCoO_2$ is a semiconductor with an electronic conductivity lower than 10^{-3} S cm^{-1} at room temperature and an activation energy close to 0.15 eV,[7] while Li_xCoO_2 at concentrations below $x = 0.75$ is metallic.[8] Both phases at $x = 0.94$ and 0.75 have very close structures in the rhombohedral system. A particular feature can be observed at $x = 0.5$ which is associated to a monoclinic distortion and results from an interslab lithium/vacancy ordering at this concentration.[4,9] Then Li_xCoO_2 undergoes other phase transitions to reach the CoO_2 hexagonal phase with O1 type packing. For Li concentrations between $x = 1$ and 0, the layered character of Li_xCoO_2 is maintained, and it was shown that 95% of the Li^+ ions can be reinserted back into CoO_2.[6]

* Corresponding author: e-mail remi.dedryvere@univ-pau.fr.
† Université de Pau.
‡ Université Bordeaux I.

(1) Mizushima, K.; Jones, P. C.; Wiseman, P. J.; Goodenough, J. B. *Mater. Res. Bull.* **1980**, *15*, 783–789.
(2) Whittingham, M. S. *Chem. Rev.* **2004**, *104*, 4271–4302.
(3) Orman, H. J.; Wiseman, P. J. *Acta Crystallogr. C* **1984**, *40*, 12–14.
(4) Reimers, J. N.; Dahn, J. R. *J. Electrochem. Soc.* **1992**, *139*, 2091–2097.
(5) Ohzuku, T.; Ueda, A. *J. Electrochem. Soc.* **1994**, *141*, 2972–2977.
(6) Amatucci, G. G.; Tarascon, J.-M.; Klein, L. C. *J. Electrochem. Soc.* **1996**, *143*, 1114–1123.
(7) Ménétrier, M.; Saadoune, I.; Levasseur, S.; Delmas, C. *J. Mater. Chem.* **1999**, *9*, 1135–1140.
(8) Molenda, J.; Stocklosa, A.; Bak, T. *Solid State Ionics* **1989**, *36*, 53–58.
(9) Shao-Horn, Y.; Levasseur, S.; Weill, F.; Delmas, C. *J. Electrochem. Soc.* **2003**, *150*, A366.

10.1021/cm702546s CCC: $40.75 © 2008 American Chemical Society
Published on Web 12/15/2007

Concerning the electrochemical reaction and the electronic transfers induced by intercalation/deintercalation of lithium in Li_xCoO_2, many investigations have also been carried out. It is very important to understand how the charge of lithium is transferred to oxygen and to the metal because $LiCoO_2$ stands as reference compound for a whole family of materials obtained by substitution of other metals for cobalt in order to improve the properties of this class of compounds as positive electrode materials for lithium ion batteries. Surprisingly, despite numerous reports on $LiCoO_2$ and careful experimental and theoretical investigations presently carried out on more complex compounds, the electron transfer mechanisms in $LiCoO_2$ itself remain a controversial topic, in such a way that additional work looks necessary to shed light on this subject.

In the initial state, cobalt in $LiCoO_2$ is in the low-spin t_{2g}^6 configuration (formally Co^{3+}).[7,8,10] To describe the Li^+ deintercalation process, the conventional concept is to assume that charge compensation concerns only the transition metal, since lithium is completely ionized and the oxygen valence is considered as fixed at O^{2-}, resulting in a change of cobalt oxidation state from Co^{3+} in $LiCoO_2$ to Co^{4+} in CoO_2. However, about a decade ago, new theoretical studies have brought this concept into question. With the help of ab initio pseudopotential calculations in the local density approximation (LDA), Ceder and co-workers[11–13] have shown that, upon intercalation of Li^+ into CoO_2, about 28% of the valence charge of lithium is transferred to cobalt, while 50% is transferred to oxygens, so that actually more charge is transferred to the oxygen ions than to the metal ions. The authors have shown that, concerning cobalt, the charge is transferred to the t_{2g} bands, while intercalation of lithium makes the Co−O bond more ionic in $LiCoO_2$ than in CoO_2. This mechanism can be considered to lead to the increase of charge found on oxygen.

Simultaneously, in other reports based on total-energy calculations by the linearized augmented plane wave (LAPW) technique within LDA, Wolverton and Zunger[14,15] state that the charge enclosed around the cobalt site remains almost constant in Li_xCoO_2 for all values $0 \leq x \leq 1$, so that the electronic charge would be almost entirely transferred to oxygen ions. More recently, Catti has reported a study on the monoclinic $Li_{0.5}CoO_2$ based on ab initio periodic Hartree–Fock calculations[16] to investigate the diffusion of Li^+ in the structure. A careful analysis of the Mulliken charges indicates that an extensive redistribution of charges occurs with respect to $LiCoO_2$, concerning both cobalt and oxygen atoms.

In spite of the quality of the models used and the remarkable significance of the conclusions that can be deduced, computational studies do not explain all the electronic properties of deintercalated phases Li_xCoO_2. For example, the accurate first-principles study of Ceder and coworkers on the phase diagram of Li_xCoO_2 could not predict the two-phase domain induced by the insulator–metal transition for $0.75 \leq x \leq 0.93$.[12]

Concerning experimental studies, numerous reports give rise to contradictory conclusions. Different authors refer to such and such calculations results to interpret their experimental results, depending on whether they observe an electron transfer to both the cobalt and the oxygen or not. Most of the studies are based on X-ray absorption spectroscopy (XAS). Several studies based on Co K-edge XAS[17,18] have evidenced a positive energy shift in the spectra of Li_xCoO_2 upon lithium deintercalation, showing the progressive oxidation of cobalt. However, they did not investigate the O K-edge. In several studies based on O K-edge, Co K-edge, and Co $L_{2,3}$-edge XAS[19,20] the authors concluded that the charge compensation for the lithium deintercalation is achieved at both the oxygen and cobalt atomic sites simultaneously, with a main part of the charge transferred to oxygen, in good agreement with theoretical results of Ceder et al.

On the other hand, in a study using O K-edge and Co $L_{2,3}$-edge XAS, Montoro et al.[21] did not observe any shift in the cobalt spectra and concluded that cobalt ions remain mostly unaffected by the lithium deintercalation. However, in this case the Li_xCoO_2 samples have been prepared by chemical delithiation in aqueous acidic solution, which can have an influence on their surface properties, with the possible presence of protons exchanged for Li ions. For example, their sensitivity toward moisture and air is much lower than electrochemically deintercalated samples. This could be the reason for the nonobservation of any effect on cobalt. Graetz et al., in an electron energy-loss spectroscopy (EELS) study,[22] have drawn the same conclusion. However, in this case too the samples have been prepared by chemical delithiation in aqueous solution.

Some of us have evidenced a gradual loss of observability of the ^{7}Li NMR signal when lithium is deintercalated from Li_xCoO_2 in the $0.94 \leq x \leq 1$ composition range.[7] This loss of observability was assigned to the presence of paramagnetic Co^{4+} ions and was considered to be enhanced by Co^{3+}/Co^{4+} electronic hopping around Li. For $x < 0.75$, a Knight-shifted ^{7}Li NMR signal was observed and was assigned to an electronic delocalization between Co^{3+} and Co^{4+} ions, leading to metallic-type conduction. The picture, as seen by NMR, is therefore oxidation of Co upon Li deintercalation. With the help of magnetic susceptibility measurements,

(10) van Elp, J.; Wieland, J. L.; Eskes, H.; Kuiper, P.; Sawatzky, G. A.; de Groot, F. M. F.; Turner, T. S. *Phys. Rev. B* **1991**, *44*, 6090–6103.
(11) Aydinol, M. K.; Kohan, A. F.; Ceder, G.; Cho, K.; Joannopoulos, J. *Phys. Rev. B* **1997**, *56*, 1354–1365.
(12) Van der Ven, A.; Aydinol, M. K.; Ceder, G. *Phys. Rev. B* **1998**, *58*, 2975–2987.
(13) Ceder, G.; Van der Ven, A.; Marianetti, C.; Morgan, D. *Model. Simul. Mater. Sci. Eng.* **2000**, *8*, 311–321.
(14) Wolverton, C.; Zunger, A. *Phys. Rev. Lett.* **1998**, *81*, 606–609.
(15) Wolverton, C.; Zunger, A. *Phys. Rev. B* **1998**, *57*, 2242–2252.
(16) Catti, M. *Phys. Rev. B* **2000**, *61*, 1795–1803.
(17) Nakai, I.; Takahashi, K.; Shiraishi, Y.; Nakagome, T.; Nishikawa, F. *J. Solid State Chem.* **1998**, *140*, 145–148.
(18) Balasubramanian, M.; Sun, X.; Yang, X. Q.; McBreen, J. *J. Electrochem. Soc.* **2000**, *147*, 2903–2909.
(19) Yoon, W.-S.; Kim, K.-B.; Kim, M.-G.; Lee, M.-K.; Shin, H.-J.; Lee, J.-M.; Lee, J.-S.; Yo, C.-H. *J. Phys. Chem. B* **2002**, *106*, 2526–2532.
(20) Chen, C.-H.; Hwang, B.-J.; Chen, C.-Y.; Hu, S.-K.; Chen, J.-M.; Sheu, H.-S.; Lee, J.-F. *J. Power Sources* **2007**, *174*, 938–943.
(21) Montoro, L. A.; Abbate, M.; Rosolen, J. M. *Electrochem. Solid State Lett.* **2000**, *3*, 410–412.
(22) Graetz, J.; Hightower, A.; Ahn, C. C.; Yazami, R.; Rez, P.; Fultz, B. *J. Phys. Chem. B* **2002**, *106*, 1286–1289.

Kellerman et al. also displayed the appearance of paramagnetic defect centers in Li_xCoO_2.[23]

Considering all these studies, it appears that additional experimental investigations are necessary to bring some new developments on this subject, all the more that none of these experimental studies have considered possible surface layers, particularly for samples obtained electrochemically. X-ray photoelectron spectroscopy (XPS) has proven to be an efficient tool to study positive and negative electrode materials for lithium ion batteries[24–27] as well as electrode/electrolyte interfaces.[28–30] In this paper, we carried out quasi-complete electrochemical lithium deintercalation from $LiCoO_2$ to Li_xCoO_2 ($x \approx 0$) and we analyzed the electron transfer mechanisms by XPS. To our knowledge, up to now such electrochemical delithiation down to $x = 0$ has been carried out only for structural studies based on X-ray diffraction measurements.[6]

Experimental Section

The starting $LiCoO_2$ materials were prepared by direct solid-state reaction from Li_2CO_3 (Alfa Aesar, minimum 99%) and Co_3O_4 (calcination at 400 °C for 12 h under O_2 of $CoCO_3$ (Alfa Aesar, minimum 99%)) with a starting Li/Co ratio of 1.0. The finely ground mixtures were pressed into pellets and heated at 600 °C for 12 h under O_2 and then crushed and reheated at 900 °C under O_2 for ca. 15 days. Such a long annealing allows to suppress any slight Li overstoichiometry, and perfectly stoichiometric $LiCoO_2$ is obtained as checked using ^{7}Li MAS NMR which shows no trace of other signal than the −0.5 ppm one.[31] No trace of Co_3O_4 or Li_2CO_3 could be detected by long exposure XRD.

Delithiation was carried out electrochemically by preparing lithium cells, in which the negative electrode was a lithium foil, the positive electrode was a sintered pellet of $LiCoO_2$ (obtained by pressing 500 mg of $LiCoO_2$ powder into a 13 mm diameter pellet under a 5 ton pressure and sintering the pellet at 800 °C for 24 h under O_2), and the electrolyte $LiPF_6$ (1 mol L^{-1}) in EC:PC:DMC. The cells were galvanostatically charged at the C/100 rate (corresponding to the removal of 0.01 Li per hour), the charge processes being interrupted after each 0.02 Li deintercalation step by relaxation periods with a stability criterion of 1 mV h^{-1}, to allow for homogenization of the Li content in the material. The deintercalated pellet samples were subsequently recovered in an argon-filled drybox, washed in dimethyl carbonate, and dried under vacuum.

To prevent the samples from moisture/air exposure on the analysis site, the XPS spectrometer was directly connected through a transfer chamber to a nitrogen drybox. To avoid any tiny surface contamination, the pellets were scraped with a scalpel blade under ultrahigh vacuum (5×10^{-7} Pa) before analysis. XPS measurements were carried out with a Kratos Axis Ultra spectrometer using a focused monochromatized Al Kα radiation ($h\nu = 1486.6$ eV). For the Ag $3d_{5/2}$ line the full width at half-maximum (fwhm) was 0.58 eV under the recording conditions. The analyzed area of the samples was 300×700 μm^2. Peaks were recorded with a constant pass energy of 20 eV. The pressure in the analysis chamber was ca. 5×10^{-7} Pa. Short acquisition time control spectra were recorded at the beginning and at the end of each experiment to check the nondegradation of the samples. The binding energy scale was calibrated from the carbon contamination using the C 1s peak at 285.0 eV. Core peaks were analyzed using a nonlinear Shirley-type background.[32] The peak positions and areas were optimized by a weighted least-squares fitting method using 70% Gaussian and 30% Lorentzian line shapes. Quantification was performed on the basis of Scofield's relative sensitivity factors.[33]

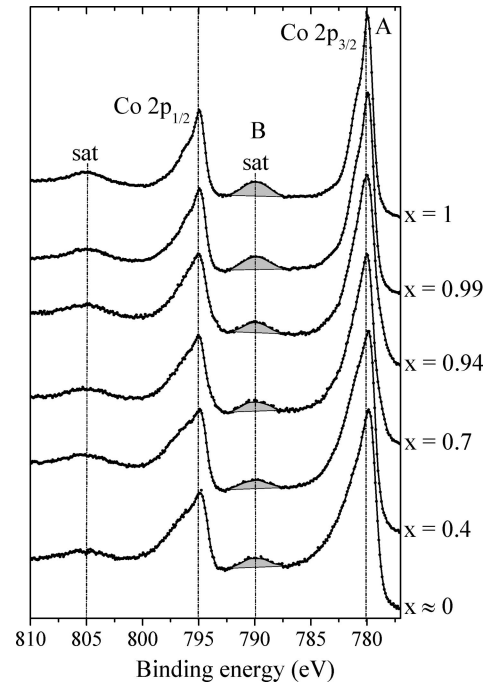

Figure 2. Co 2p XPS core peaks of Li_xCoO_2 ($0 \leq x \leq 1$).

Results and Discussion

In order to investigate redox mechanisms occurring upon lithium deintercalation in $LiCoO_2$, various Li_xCoO_2 samples ($x = 1$, 0.99, 0.94, 0.7, 0.4, 0) corresponding to different battery states of charge have been studied by XPS.

Co 2p Core Peaks. Figure 2 shows the Co 2p core peaks of these six samples. Because of spin–orbit coupling, each spectrum is split in two parts (Co $2p_{3/2}$ and Co $2p_{1/2}$), with an intensity ratio close to 2/1. Each part consists of a main line A and a satellite peak B. The starting compound $LiCoO_2$ shows a Co $2p_{3/2}$ main line at 780 eV with a satellite peak at 790 eV and a Co $2p_{1/2}$ main line at 795 eV with a satellite peak at 805 eV. The presence of a main line together with a satellite peak (shake-up) results from a ligand-to-metal

(23) Kellerman, D. G.; Galakhov, V. R.; Semenova, A. S.; Blinovskov, Ya. N.; Leonidova, O. N. *Phys. Solid State* **2006**, *48*, 548–556.
(24) Dedryvère, R.; Laruelle, S.; Grugeon, S.; Poizot, P.; Gonbeau, D.; Tarascon, J.-M. *Chem. Mater.* **2004**, *16*, 1056–1061.
(25) Lindic, M. H.; Martinez, H.; Benayad, A.; Pecquenard, B.; Vinatier, P.; Levasseur, A.; Gonbeau, D. *Solid State Ionics* **2005**, *176*, 1529–1537.
(26) Benayad, A.; Martinez, H.; Gies, A.; Pecquenard, B.; Levasseur, A.; Gonbeau, D. *J. Electron Spectrosc. Relat. Phenom.* **2006**, *150*, 1–10.
(27) Blyth, R. I. R.; Buqa, H.; Netzer, F. P.; Ramsey, M. G.; Besenhard, J. O.; Golob, P.; Winter, M. *Appl. Surf. Sci.* **2000**, *167*, 99–106.
(28) Herstedt, M.; Abraham, D. P.; Kerr, J. B.; Edström, K. *Electrochim. Acta* **2004**, *49*, 5097–5110.
(29) Dedryvère, R.; Gireaud, L.; Grugeon, S.; Laruelle, S.; Tarascon, J.-M.; Gonbeau, D. *J. Phys. Chem. B* **2005**, *109*, 15868–15875.
(30) Dedryvère, R.; Laruelle, S.; Grugeon, S.; Gireaud, L.; Tarascon, J.-M.; Gonbeau, D. *J. Electrochem. Soc.* **2005**, *152*, A689–A696.
(31) Levasseur, S.; Ménétrier, M.; Shao-Horn, Y.; Gautier, L.; Audemer, A.; Demazeau, G.; Largeteau, A.; Delmas, C. *Chem. Mater.* **2003**, *15*, 348–354.
(32) Shirley, D. A. *Phys. Rev. B* **1972**, *5*, 4709.
(33) Scofield, J. H. *J. Electron Spectrosc. Relat. Phenom.* **1976**, *8*, 129–137.

Table 1. Satellite Relative Area (%) and Full Width at Half-Maximum (eV) of the Main Peak from Co $2p_{3/2}$ Spectra of Delithiated Li_xCoO_2 Samples

	% sat. area	fwhm (eV)
$LiCoO_2$	9.1	1.9
$Li_{0.99}CoO_2$	8.3	2.1
$Li_{0.94}CoO_2$	5.3	2.6
$Li_{0.7}CoO_2$	5.2	2.6
$Li_{0.4}CoO_2$	4.6	3.1
CoO_2	4.6	3.2

charge transfer during the photoemission process and can be interpreted, at the simplest level of approximation, by a molecular orbital description.[34–36] In the initial state $LiCoO_2$ has six electrons in the cobalt 3d shell and a filled ligand shell L (oxygen 2p shell), which can be written $2p^63d^6L$. The Co 2p photoemission process can lead to several final states after creation of the 2p core hole ($2p^5$). The main line A is mainly characterized by the $2p^53d^7L^{-1}$ configuration, where one electron is transferred from the ligand shell L to the metal 3d shell (screening effect), resulting in a $3d^7$ configuration. The shake-up satellite B can be assigned to $2p^53d^6L$ and $2p^53d^8L^{-2}$ configurations.

The Co $2p_{3/2}$ main line also displays a weak shoulder at 781 eV. This fine structure can also be noticed on the Co $2p_{1/2}$ component by the presence of a shoulder at 796 eV. This feature cannot be explained by a small amount of Co^{2+} ions because Co^{2+} in oxygen environment is characterized by a strong broadening of the main line and a very intense satellite peak at 786 eV (Co $2p_{3/2}$) and 803 eV (Co $2p_{1/2}$), which is not observed here.[37] This shoulder would rather be explained by a final state effect of the photoemission process like in the case of NiO (nonlocal screening).[38,39] This fine structure was not observed in the early XPS studies of $LiCoO_2$[40–43] and can be detected only with the latest generation of spectrometers that allow better spectral resolution.

When lithium is deintercalated from Li_xCoO_2, the overall shape of the Co 2p core peak is retained. However, although the binding energies of both the main peak and the satellite remain unchanged, two important modifications can be noticed: (i) a significant broadening of the main peak toward the higher binding energies and (ii) a strong decrease of the satellite peak relative area. The changes of both parameters have been reported in Table 1. Upon lithium deintercalation the full width at half-maximum (fwhm) of the Co $2p_{3/2}$ main peak increases from 1.9 to 3.2 eV and the relative satellite peak area decreases from 9.1% to 4.6%. Both the binding energy and the relative area of the satellite peak are a more efficient tool to access the oxidation state of cobalt than the binding energy of the main peak itself. Indeed, the position and intensity of the satellite peak are highly dependent on the nature and number of the ligands and on the metal oxidation state. For example, although Co^{3+} and Co^{2+} in oxygen environment have very close main peak positions (780.0 and 780.3 eV, respectively), their satellite peaks are very different, with a binding energy of 790 eV and a relative area of 9% for Co^{3+} and a binding energy of 786 eV and a relative area of 33% for Co^{2+}.[24]

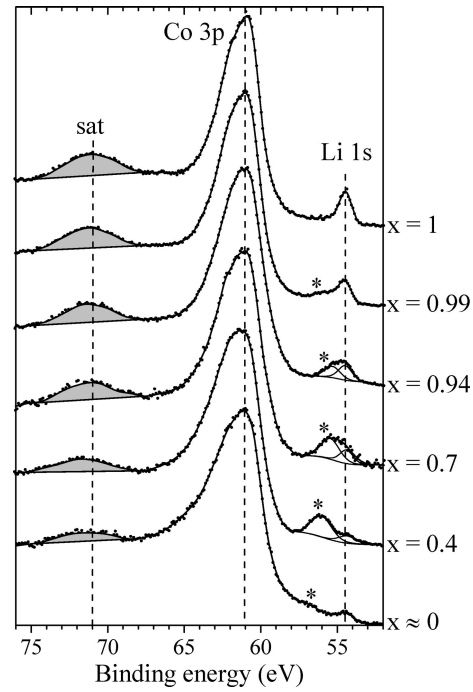

Figure 3. Co 3p and Li 1s core peaks of Li_xCoO_2 ($0 \le x \le 1$) (* = LiF and other constituents of the surface layer).

Therefore, the relative intensity of the shake-up satellite observed in Figure 2 is an essential parameter to check the evolution of the cobalt oxidation state. To our knowledge, the precise energy position and the relative intensity of the shake-up satellite characteristic for Co^{4+} ions in oxygen environment have not been reported. However, it is obvious that the strong decrease of the relative satellite area (from 9.1% to 4.6%) observed in Figure 2, together with the strong broadening of the main peak, can be attributed to an oxidation process (at least partial) of Co^{3+}.

Moreover, a disproportionation mechanism of $LiCoO_2$ to form both CoO_2 and Co_3O_4, as sometimes assumed,[44] can be excluded because the characteristic satellite peak of Co^{2+} in oxygen environment is not observed.

Co 3p Core Peaks. Figure 3 shows the Co 3p XPS core peaks of the same samples. The $3p_{3/2}-3p_{1/2}$ splitting is too small to be observed. As for Co 2p, the Co 3p spectrum of the starting compound $LiCoO_2$ consists of a main line and a shake-up satellite (at 61 and 71 eV, respectively). Upon lithium deintercalation we can observe a strong decrease of

(34) Hüfner, S. *Photoelectron Spectroscopy: Principles and Applications*; Springer-Verlag: Berlin, 1995.
(35) Fadley, C. S. *Electron Spectroscopy: Theory, Techniques and Applications*; Brundle, C. R., Baker, A. D., Eds.; Academic Press: New York, 1978.
(36) Hüfner, S. *Adv. Phys.* **1994**, *43*, 183–356.
(37) Kim, K. S. *Phys. Rev. B* **1975**, *11*, 2177–2185.
(38) Van Veenendaal, M. A.; Sawatzky, G. A. *Phys. Rev. Lett.* **1993**, *70*, 2459.
(39) Van Veenendaal, M. A.; Heskes, H.; Sawatzky, G. A. *Phys. Rev. B* **1993**, *47*, 11462.
(40) Oku, M. *J. Solid State Chem.* **1978**, *23*, 177.
(41) Kemp, P.; Kox, P. A. *J. Phys.: Condens. Matter* **1990**, *2*, 9653.
(42) Galakhov, V. R.; Karelina, V. V.; Kellerman, D. G.; Gorshkov, V. S.; Ovechkina, N. A.; Neumann, M. *Phys. Solid State* **2002**, *44*, 266–273.
(43) Dupin, J.-C.; Gonbeau, D.; Martin-Litas, I.; Vinatier, P.; Levasseur, A. *J. Electron Spectrosc. Relat. Phenom.* **2001**, *120*, 55–65.
(44) Aurbach, D.; Markovsky, B.; Salitra, G.; Markevich, E.; Talyossef, Y.; Koltypin, M.; Nazar, L.; Ellis, B.; Kovacheva, D. *J. Power Sources* **2007**, *165*, 491–499.

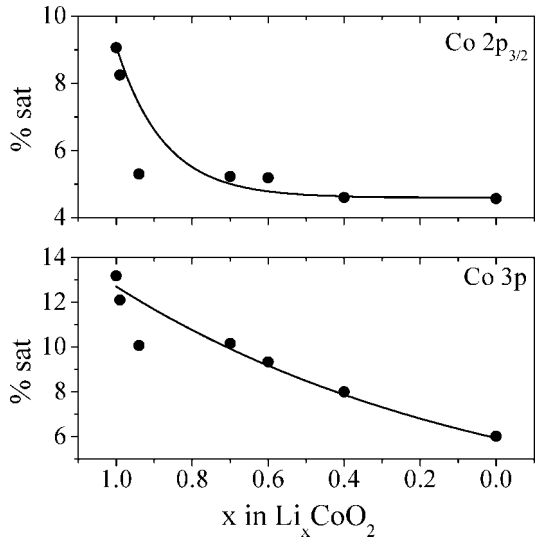

Figure 4. Satellite relative area (%) from Co $2p_{3/2}$ and Co 3p core peaks of Li_xCoO_2.

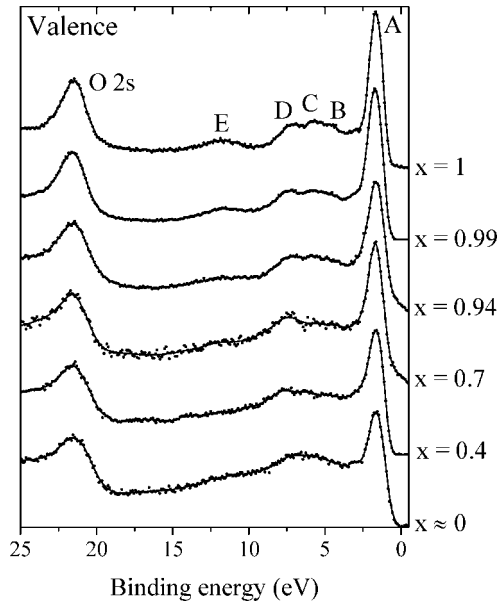

Figure 5. XPS valence spectra of Li_xCoO_2 ($0 \leq x \leq 1$).

the satellite relative area from 13.2% to 6.0%, together with a strong broadening of the main peak toward higher binding energies. This observation confirms the oxidation process of Co^{3+}.

The two cobalt signals provide complementary information, and it is interesting to compare the changes of the satellite relative area for Co 2p and Co 3p core peaks, as shown in Figure 4. For both signals the overall trend is the same: the satellite intensity is divided by two from $LiCoO_2$ to CoO_2 (from 9.1 to 4.6% for Co 2p, from 13.2 to 6.0% for Co 3p). The difference is that the satellite intensity decrease upon delithiation is much stronger for Co 2p than for Co 3p. This can be explained by the analysis depth associated to each XPS signal. The kinetic energy of the photoelectrons coming into the analyzer is about 700 eV for Co 2p and 1420 eV for Co 3p, resulting in a photoelectron escape depth about 1.5 times greater for Co 3p than for Co 2p. Therefore, Co 3p core peak is more representative of the bulk material than Co 2p. This could explain why the decrease observed for Co 3p is more gradual and closer to linearity vs the lithium amount x in Li_xCoO_2 determined by electrochemistry (Figure 4), if one considers that Co^{3+} ions are more oxidized at the extreme surface of the material, probably due to lithium deficiency at the very surface. It is worth noting that such a difference in behavior of surface and bulk has been very recently highlighted by Chen et al.[20] concerning oxygen in Li_xCoO_2 ($0.64 < x < 1$). In their study based on O K-edge XAS using two different detection modes (total electron yield and fluorescence) corresponding to different analysis depths, the authors have shown that the electron charge transfer to oxygen atoms is more obvious at the surface of the material than in the bulk. However, in this case the samples have been prepared by chemical delithiation in aqueous solution.

Valence Spectra. The analysis of XPS valence bands also provides additional information. Figure 5 shows valence spectra of $LiCoO_2$ and delithiated samples. The valence spectrum of starting $LiCoO_2$ can be interpreted on the basis of band structure calculations carried out by Czyzyk et al. (localized spherical waves LSW method).[45] The narrow intense peak A at 1.7 eV is mainly assigned to Co 3d states (t_{2g}). Component B at 4.4 eV is mainly assigned to O 2p states, peak C at 5.7 eV results from interactions of O 2p and Co 3d states, and peak D at 7.3 eV results from interactions of O 2p and Co 4s−4p states. Peak E at 11.7 eV cannot be predicted by band structure calculations and is attributed to a shake-up satellite.[10,41] Finally, the peak at 21.5 eV corresponds to O 2s states.

Changes in the valence spectra as shown in Figure 5 allow us to check changes in the electronic structure of Li_xCoO_2 that may occur upon lithium deintercalation. All spectra have been normalized with respect to the O 2s peak, taking into account that the measured Co 2p/O 1s ratio of Li_xCoO_2 remains roughly constant. The trend for the spectra of delithiated samples clearly displays a decrease of peak A, which is particularly significant for low lithium contents $x = 0.4$ and $x \approx 0$. This change can be explained by a decrease of the electron population of the Co 3d states, ensuing from the creation of holes in the t_{2g} band formed by overlapping t_{2g} orbitals of Co in octahedra sharing edges. Partial filling of this band leads to the itinerant character of the electrons and the metallic character of the $x < 0.75$ samples. This observation therefore confirms partial oxidation of Co^{3+}, in good agreement with the analysis of Co 2p and Co 3p core peaks. This modification of the valence band was not detected in the earlier study of Kellerman et al. in the same kind of study,[23] probably because lithium was deintercalated only down to $x = 0.6$.

Note that our study of valence spectra was possible here because they are very weakly disturbed by other compounds formed at the electrode/electrolyte interface, resulting from degradation reactions of electrolyte constituents. The very weak contribution of these species to the valence spectrum is certainly due to the thinness of the surface layer and to

(45) Czyzyk, M. T.; Potze, R.; Sawatzky, G. A. *Phys. Rev. B* **1992**, *46*, 3729–3735.

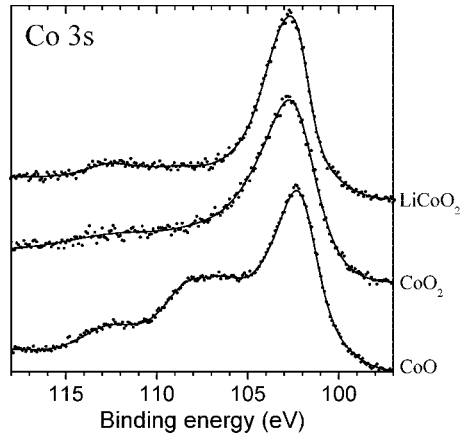

Figure 6. Co 3s core peaks of $LiCoO_2$, CoO_2, and CoO.

the greater analysis depth of valence spectra as compared to core peaks (kinetic energy of the valence photoelectrons ≈1480 eV).

Co 3s Core Peaks. Once the oxidation process of cobalt has been evidenced, the question of the spin state (high spin or low spin) of cobalt in Li_xCoO_2 can be investigated. In the initial $LiCoO_2$ material, Co^{3+} is in the low-spin t_{2g}^6 configuration. M 3s core peaks of transition metals M are very sensitive to the metal spin state. Indeed, when the 3d spin is different from zero, the spectrum consists of two components resulting from the exchange interaction of M 3s and 3d electrons, leading to an energy difference between two photoemission final states with the 3s spin parallel or antiparallel to the 3d spin. The magnitude of the M 3s splitting is proportional to $(2S+1)K(3s,3d)$, where S is the value of the local 3d spin and $K(3s,3d)$ is the Slater exchange integral between the 3s and the 3d electrons.[34] The shape of M 3s spectra also depends on ligand-to-metal charge transfer phenomena.[46,47] Figure 6 shows Co 3s spectra of $LiCoO_2$, of the quasi-fully delithiated CoO_2, and of CoO for comparison. The spectrum of starting $LiCoO_2$ displays a main peak at 102.7 eV and satellite peaks in the 106–115 eV binding energy region. The main peak does not display any splitting due to the low-spin configuration ($S = 0$) of Co^{3+} in $LiCoO_2$. A very different shape is observed for CoO. The complex structure of its Co 3s spectrum results, beside charge transfer phenomena, from a strong splitting due to the $3d^7$ high-spin configuration of Co^{2+} ($S = 3/2$). The spectrum of quasi-fully delithiated CoO_2 displays a significant broadening with respect to $LiCoO_2$ (4.3 eV instead of 3.1 eV) but no complex structure as in the case of CoO. It is in good agreement with a weak splitting due to a $3d^5$ low-spin configuration of Co^{4+} ($S = 1/2$) and allows us to exclude the high-spin configuration $S = 5/2$ that would result in a much greater splitting of the Co 3s spectrum.

These results are in good agreement with those of Kellerman et al.[23] On the basis of magnetic susceptibility measurements, the authors also concluded that the low-spin state of cobalt in Li_xCoO_2 was the most probable configuration because the high-spin configuration would lead to much greater experimental magnetic moment values. Moreover, they found that magnetic moments measured for Li_xCoO_2 were even smaller than expected for Co^{4+} ions having only one unpaired d electron. To explain this result, the authors proposed that lithium deintercalation from $LiCoO_2$ induces not only a change in the electronic state of cobalt but also a partial oxidation of oxygen ions ($O^{2-} \rightarrow O^{-2+\delta}$) (note that weak Pauli-type susceptibility is expected for such metallic samples, which would also explain the weak magnetic response observed by the authors). So we decided to carefully analyze O 1s core peaks to grasp more insight into the oxidation state of oxygen.

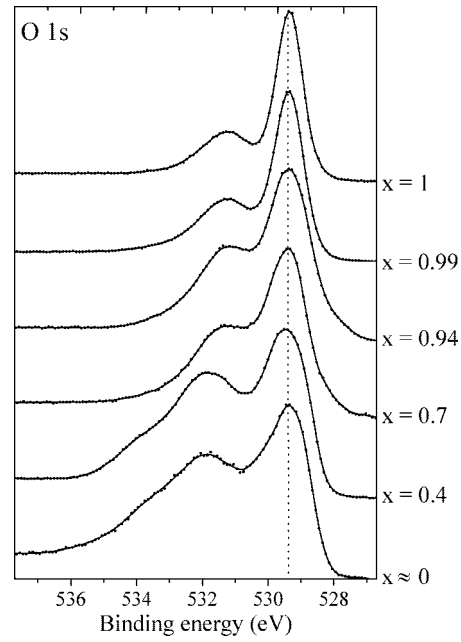

Figure 7. O 1s core peaks of Li_xCoO_2 ($0 \leq x \leq 1$).

O 1s Core Peaks. Figure 7 shows O 1s core peaks of $LiCoO_2$ and lithium-deintercalated samples. The spectrum of starting $LiCoO_2$ displays a characteristic profile including two peaks. The narrow peak at 529.7 eV is characteristic of O^{2-} anions of the crystalline network. The second peak at higher binding energy (531.6 eV) may be assigned to weakly absorbed species at the surface; however, the contamination is very weak here, and this peak is more probably due to oxygen anions of $LiCoO_2$ in the subsurface, which have a deficient coordination. This behavior is commonly observed with oxides.[48]

When lithium is deintercalated from $LiCoO_2$, we can observe a gradual enhancement of the higher binding energy components. Simultaneously, the ratio between the $LiCoO_2$ lattice O 1s signal (529.7 eV) and the Co 2p signal remains roughly constant. Thus, the enhancement of the higher binding energy O 1s components cannot be assigned to Li_xCoO_2 but to additional oxygen-containing species formed at the electrode/electrolyte interface upon the electrochemical reaction and resulting from the degradation of electrolyte constituents. Numerous works have dealt with the charac-

(46) Kinsinger, V.; Zimmermann, R.; Hüfner, S.; Steiner, P. *Z. Phys. B: Condens. Matter* **1992**, *89*, 21.
(47) Bagus, P. S.; Freund, H. J.; Minerva, T.; Pacchioni, G.; Parmigiani, F. *Chem. Phys. Lett.* **1996**, *251*, 90.
(48) Dupin, J.-C.; Gonbeau, D.; Vinatier, P.; Levasseur, A. *Phys. Chem. Chem. Phys.* **2000**, *2*, 1319–1324.

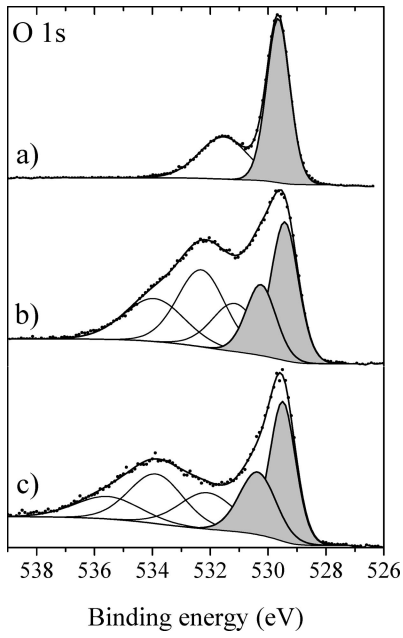

Figure 8. O 1s core peaks of (a) $LiCoO_2$ and (b, c) CoO_2 in different experimental conditions (see text).

terization of organic and inorganic species formed in the passivation film at the surface of Li ion battery electrodes, and several degradation mechanisms of the salt $LiPF_6$ and the carbonated solvents can be found elsewhere.[49–51] In Figure 7 we can notice a change of the curve shape at $x = 0.4$ and $x \approx 0$ with the appearance of a new component at high binding energy (about 534 eV). This is probably due to additional species deposited at the electrode surface and resulting from oxidation mechanisms of the solvents because of the very high potentials that are reached to extract lithium down to $Li_{0.4}CoO_2$ (4.3 V) and CoO_2 (5.2 V).

An other important feature that can be noticed in Figure 7 is the strong broadening of the Li_xCoO_2 lattice O 1s signal toward higher binding energies. Indeed, for $x = 0.4$ and $x \approx 0$ the peak at 529.7 eV displays a very asymmetrical shape. This feature has been analyzed more carefully in Figure 8, which presents the O 1s spectra of (a) the starting $LiCoO_2$ material, (b) CoO_2, and (c) CoO_2 in special experimental conditions (charge neutralization) that allow to shift the components of oxygenated species formed at the interface with respect to the CoO_2 component itself. Indeed, during the XPS experiment, the emission of photoelectrons entails a loss of negative charge, which is usually balanced by supplying low kinetic energy electrons from a charge neutralizer. However, when a sample is made up of mixed conducting and insulating compounds, it is commonly observed that the signals of each type of compound are shifted differently (differential charging effect). Particularly, this may be observed when an insulating film is present at the surface of a conducting substrate, like for Li ion battery electrodes for example. Normally, this differential charging effect must be minimized by an adequate sample preparation and a careful adjustment of the charge neutralizer. This is the case for spectrum b of CoO_2. On the contrary, for spectrum c of CoO_2 the differential charging effect has been exaggerated in order to shift significantly all the peaks assigned to compounds of the electrode/electrolyte interface and to separate the O 1s signals of CoO_2 from those of the interface constituents. A comparison between spectra b and c allows to clearly display the asymmetrical shape of the CoO_2 lattice O 1s signal. This peak broadening toward the higher binding energies with respect to $LiCoO_2$, represented here by a second peak at 530.3 eV, can be interpreted by a partial oxidation process of O^{2-} ions from $LiCoO_2$ to CoO_2. This study confirms the hypothesis that both cobalt and oxygen undergo oxidation-type changes in their electronic structure when lithium ions are deintercalated from $LiCoO_2$. Although the Co t_{2g} orbitals are often considered in first approximation as nonbonding, it is indeed reasonable to consider that decreasing their electron occupation is also somewhat felt by oxygen, be it via an increase of the covalence of the O(2p)−Co(e_g) bond, as suggested by the observed shortening of the Co−O distance upon Li deintercalation.[7]

It is worth to notice that the analysis of the oxidation state of oxygen is possible by XPS in this study because it allows to clearly distinguish the O 1s signature of the Li_xCoO_2 material itself from the components of the oxygenated species at the interface. These species can be present at the electrode surface due to electrolyte degradation reactions. Therefore, when using a surface-sensitive technique, it is necessary to consider the presence of the electrode/electrolyte interface in the study of the electrode material itself.

F 1s, P 2p, C 1s, and Li 1s Core Peaks. Figure 9 shows F 1s, P 2p, and C 1s spectra of Li_xCoO_2 ($x \approx 0$). These spectra provide additional information about compounds of the electrode/electrolyte interface. The F 1s spectrum consists of two components. The first one at 684.9 eV is attributed to lithium fluoride LiF, which is a common constituent of electrode surfaces in Li ion batteries using $LiPF_6$ as salt in the electrolyte. Several formation mechanisms of LiF from the degradation of $LiPF_6$ can be found in the numerous reports dealing with electrode/electrolyte interfaces, particularly the famous solid electrolyte interphase (SEI) formed on the graphite electrode.[50,52,53] Note that LiF can be observed in the Li 1s spectra (at 56 eV, see Figure 3) together with other lithium-containing compounds of the interface, particularly for Li_xCoO_2 compounds with $x = 0.7$ and 0.4.

The second F 1s component at 687.9 eV could be assigned to remaining traces of $LiPF_6$ that were not dissolved by washing with the solvent DMC after battery opening. Actually parallel analysis of the P 2p spectrum shows that $LiPF_6$ has completely deteriorated and that this component should be rather assigned to fluorophosphates. Indeed, the P 2p spectrum shows two unresolved doublets ($2p_{3/2}-2p_{1/2}$). The first one ($2p_{3/2}$ at 134.6 eV) can be attributed to phosphates resulting from the complete degradation of $LiPF_6$.

(49) Aurbach, D.; Markovsky, B.; Weissman, I.; Levi, E.; Ein-Eli, Y. *Electrochim. Acta* **1999**, *45*, 67–86.
(50) Vetter, J.; Novák, P.; Wagner, M. R.; Veit, C.; Möller, K.-C.; Besenhard, J. O.; Winter, M.; Wohlfahrt-Mehrens, M.; Vogler, C.; Hammouche, A. *J. Power Sources* **2005**, *147*, 269–281.
(51) Andersson, A. M.; Abraham, D. P.; Haasch, R.; MacLaren, S.; Liu, J.; Amine, K. *J. Electrochem. Soc.* **2002**, *A 149*, 1358–1369.
(52) Peled, E. *J. Electrochem. Soc.* **1979**, *126*, 2047.
(53) Aurbach, D. *J. Power Sources* **2000**, *89*, 206–218.

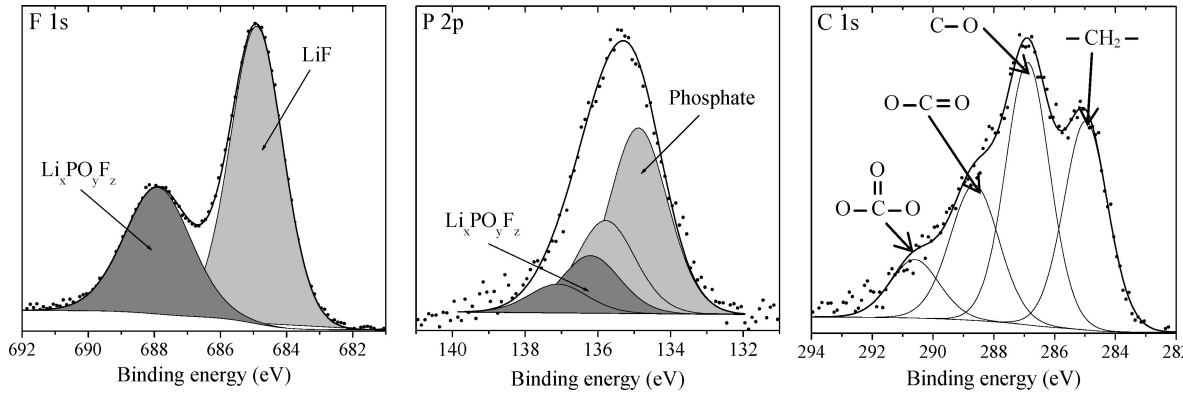

Figure 9. F 1s, P 2p, and C 1s core peaks of quasi-fully delithiated sample CoO_2.

The second one ($2p_{3/2}$ at 135.7 eV) corresponds to a lower binding energy than that expected for $LiPF_6$ (136.8–137 eV) and thus can be attributed to intermediate degradation products $Li_xPO_yF_z$ (fluorophosphates).

The C 1s spectrum of the same sample shows four components. The first one at 285.0 eV is attributed to hydrocarbon contamination and also to aliphatic carbon atoms that may result from solvent decomposition. The three other components at 286.8, 288.6, and 290.4 eV can be assigned to C−O, COO, and CO_3-like carbon environments, respectively. These components suggest the formation of organic compounds resulting from electrolyte solvents degradation. Several formation mechanisms of these species can be found in the literature.[29,49,53] However, most of these reported mechanisms are reduction reactions occurring at the surface of the negative electrode, as for example the formation of Li_2CO_3 or lithium alkyl carbonates $ROCO_2Li$ from the reduction of carbonated solvents. Therefore, the formation of carbonaceous compounds at the surface of the positive electrode Li_xCoO_2 may be explained either by oxidation mechanisms of solvents or by the migration of these species from the negative to the positive electrode following their formation by a reduction mechanism at the surface of the negative electrode. A complete identification of species that are formed at the electrode/electrolyte interface is not our aim here, but the presence of these oxygenated species allows to explain the shape of O 1s spectra previously observed in Figure 7 (components at 531–534 eV).

The overall amount of carbon measured by XPS for CoO_2 is about 11%, which is very low. Similar carbon contents were measured for all Li_xCoO_2 samples (between 9% and 16%). This result shows that the film formed at the surface of the electrode upon electrochemical charge is rather thin and explains why a detailed analysis of the Li_xCoO_2 material itself was possible in this work. If this surface film was thicker, the intensity of Li_xCoO_2 cobalt and oxygen signals would be much weaker. It is therefore necessary to consider the presence of the electrode/electrolyte interface in this kind of study.

Conclusion

In this work, we have investigated the changes in the electronic structure of $LiCoO_2$ upon lithium deintercalation. The Li^+ deintercalation was carried out electrochemically from starting material $LiCoO_2$ down to quasi-fully delithiated CoO_2. We have taken into account all available XPS core peaks and valence spectra to analyze both the electrode material itself and the electrode/electrolyte interface. The results allowed us to show that the electron charge transfer resulting from Li^+ extraction concerns simultaneously cobalt and oxygen, which both can be considered to undergo a partial oxidation process. The possibility of the sole participation of oxygen atoms to the charge transfer process can thus be ruled out. These results support the existence of a strong electronic delocalization during the delithiation of $LiCoO_2$. Moreover, we could evidence the formation of a film at the electrode/electrolyte interface upon the electrochemical reaction, which consists of organic and inorganic species resulting from the degradation of salt and solvents of the electrolyte.

This study will allow us to better understand the electron transfer mechanisms occurring in more complex layered oxides that are contemplated as possible positive electrode materials for lithium ion batteries.

Acknowledgment. The authors thank Laurence Croguennec and Dany Carlier (ICMCB) for useful discussions and Région Aquitaine for financial support.

CM702546S